

# Electrical properties of sol–gel processed PLZT thin films

J. M. KIM, D. S. YOON, K. NO

*Department of Ceramic Science and Engineering, Korea Advanced Institute of Science and Technology, Kusong Dong 373-1, Yuseong Gu, Taejeon, Korea*

Sol–gel processed lanthanum-modified lead zirconate titanate (PLZT) thin films consisting of two different perovskite phase contents were fabricated on indium tin oxide coated Corning 7059 glass substrates with two different heating schedules: direct insertion at 650° C for 30 min and at 500° C for 2 h. Optical transmittance spectra, polarization versus electric field curves, relative dielectric constant versus frequency and capacitance versus d.c. bias voltage curves of the samples were investigated. The samples showed a good transparency of over 70% and interference oscillation. A thin film consisting of mainly perovskite phase showed a slim loop hysteresis in the polarization versus electric field curve and in the capacitance versus d.c. bias voltage curve, indicating the presence of ferroelectric domains, but a film consisting of mainly pyrochlore phase did not. The dielectric constant and loss factor of the thin film consisting of mainly perovskite phase were about 90 and about 0.2, respectively, at relatively low frequency and showed dispersion of the dipolar polarization of permanent dipole moment in the ferroelectric perovskite phase in the frequency range between 10 kHz and 1 MHz.

## 1. Introduction

Lanthanum-modified lead zirconate titanate (PLZT) thin films have attracted much interest due to their potential ferroelectric, piezoelectric, pyroelectric and electro-optic properties [1–3]. Possible applications of ferroelectric PLZT thin films include ferroelectric random access memory (FRAM), waveguide modulators, display and other electro-optic devices. Earlier work on the fabrication of PLZT thin films was mainly based on vacuum deposition techniques such as ion beam deposition and sputtering [4–6]. However, problems of poor stoichiometry control and the complex set of deposition parameters in vacuum techniques have hindered the deposition of device-quality films [7]. In recent years there has been much interest in the fabrication of oxide films using the chemical sol–gel technique [8–15]. The sol–gel processing technique offers a number of advantages over conventional vacuum deposition. These include better stoichiometric control and homogeneity, processing at relatively low temperatures, larger films and lower cost.

PLZT thin films usually consist of a mixture of perovskite and pyrochlore phases. The perovskite phase possesses desirable ferroelectric properties, but the pyrochlore phase does not because the pyrochlore structure is centrosymmetric [16]. The electric properties measured in PLZT thin films are some combination of the properties of perovskite and pyrochlore phases [17], and the thin films usually show poor ferroelectric properties compared to the bulk ceramics. Being deposited on glass and indium tin oxide (ITO) coated glass substrates, the thin films cannot be heat-treated at high temperatures due to possible

degradation of the substrate, so it is difficult to get thin films having an almost pure perovskite phase. Recently, fast heating processes such as rapid thermal annealing (RTA) [18] and direct insertion [8] have been found to be excellent methods of increasing the perovskite phase content in thin films. The fast heating process has an advantage over the normal process because the duration can be significantly decreased in the relatively low temperature region at which the pyrochlore phase is stable.

The objectives of this study were to fabricate PLZT thin films having different perovskite phase contents on ITO-coated glass using direct insertion of the sol–gel processed films at different temperatures, to measure the electrical and optical properties of the thin films, and to speculate on the differences in the observed properties.

## 2. Experimental procedure

Fig. 1 illustrates a flow chart for the stock solution and thin film preparation procedure of the sol–gel process used in this study. Lead acetate  $\text{Pb}(\text{CH}_3\text{COO})_2 \cdot 3\text{H}_2\text{O}$ , lanthanum acetate  $\text{La}(\text{CH}_3\text{COO})_3 \cdot 1.5\text{H}_2\text{O}$ , zirconium n-propoxide  $\text{Zr}(\text{C}_3\text{H}_7\text{O})_4$  and titanium isopropoxide  $\text{Ti}[(\text{CH}_3)_2\text{CHO}]_4$  were used as precursors. The solution concentration was 9, 65 and 35% for La, Zr and Ti, respectively (denoted 9/65/35) and the solution consisted of 5 mol % excess Pb. Methoxyethanol ( $\text{CH}_3\text{OCH}_2\text{CH}_2\text{OH}$ ) was used as a solvent, nitric acid as a catalyst and ethylene glycol as an additive in order to prevent cracking and to improve the surface smoothness of the film. A detailed description of the process was reported in an earlier paper [8].

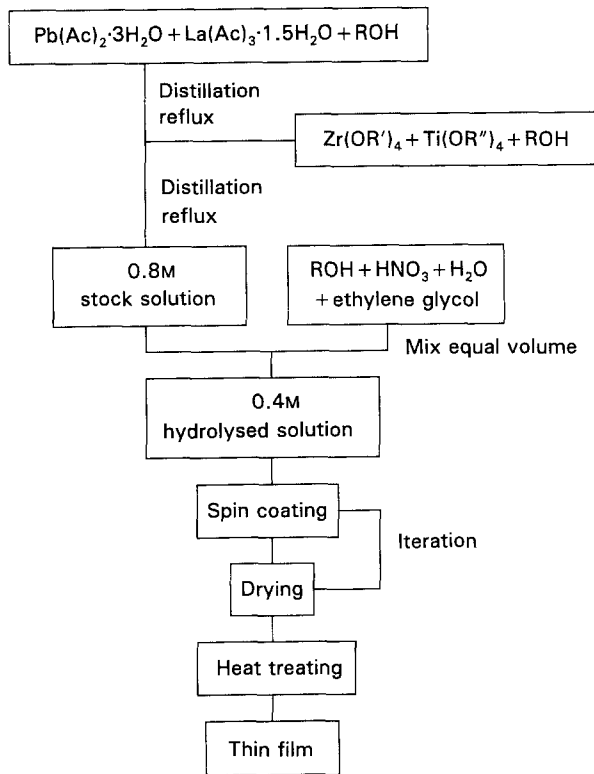


Figure 1 Experimental procedure of PLZT thin film preparation using the sol-gel method.

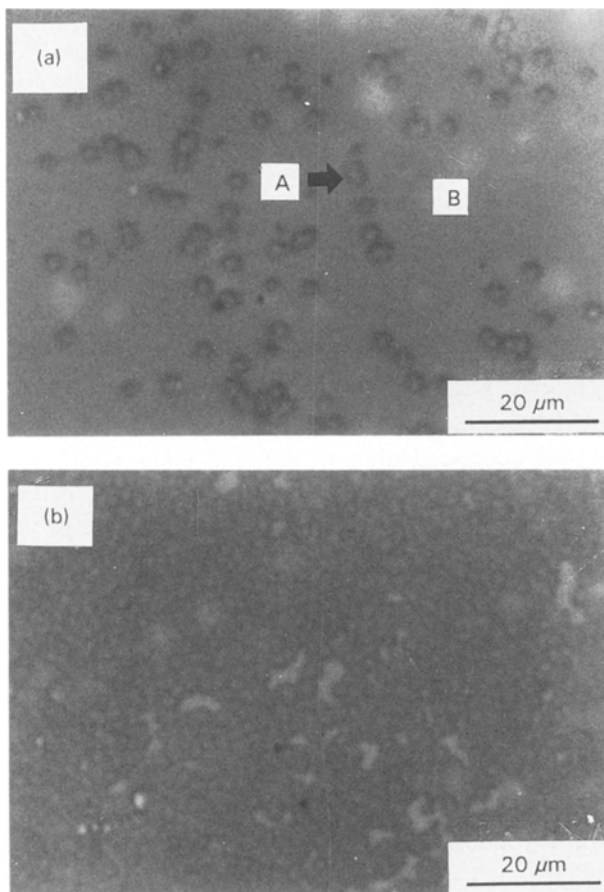


Figure 2 Microstructures of (a) PY and (b) PE samples: (A) perovskite phase, (B) pyrochlore phase.

Thin films were deposited using spin-coating of the precursor solution on ITO-coated Corning 7059 glass substrates at 3000 r.p.m. for 30 s and then dried at

350° C for 8 min. This procedure was repeated in order to obtain a film thickness of approximately 0.5 μm. The thickness of a single layer after drying was about 80 nm. The films were heat-treated with two different heating schedules: (i) inserted directly into a 500° C furnace, held at 500° C for 2 h and directly pulled out to fabricate a film consisting of mainly pyrochlore phase, and (ii) inserted directly into a 650° C furnace, held at 650° C for 30 min and directly pulled out to fabricate a film consisting of mainly perovskite phase. These heating schedules were performed in an air atmosphere. PE and PY indicate the films heat-treated at 650 and 500° C, respectively, in the following discussion.

The microstructure of the thin films was observed using an optical microscope, and the perovskite phase content was determined by counting the perovskite grains in the microstructure. The transmittance of the thin film was measured using a diode array spectrophotometer (Hewlett-Packard 8452A). The ITO layer was used for a bottom electrode, and Au spots of 1 mm diameter were deposited using sputtering for the top electrodes. The hysteresis loop of the thin film was measured using a standardized ferroelectric test system (Radiant Technologies RT-66A). The capacitance versus a.c. frequency ( $C-f$ ) and the capacitance versus bias voltage ( $C-V$ ) characteristics of the thin film were measured using an impedance analyser (Hewlett-Packard 4192A).

### 3. Results and discussion

Fig. 2 shows the microstructures of PLZT thin films (composition 9/65/35) prepared with two different heating schedules. The circular features in the microstructure are the perovskite phase (known as a rosette structure) and the remaining area surrounding the circular features consists of the pyrochlore phase [8]. The microstructure of the thin film heat-treated at 500° C for 2 h (Fig. 2a, PY sample) consists of mainly pyrochlore phase and has a relatively low perovskite phase content (approximately 10%). The microstructure of the thin film heat-treated at 650° C for 30 min (Fig. 2b, PE sample) consists of mainly perovskite phase (approximately 90%) and relatively lower pyrochlore phase content. These observations are consistent with the observations made in the other studies [8]: a high perovskite content in the PLZT film requires heat-treatment at a relatively high temperature and for short duration in order to decrease the content of the pyrochlore phase.

The optical transmittance of the PLZT thin films was measured in the wavelength range 190–820 nm. Fig. 3 shows the transmittance spectra of the ITO-coated glass substrate for comparison and the thin films heat-treated in two different heating schedules. The substrate shows over 85% transmittance without significant interference oscillation in the transmittance spectra. Interference oscillation was due to phase retardation between the reflected light beams at the surface and at the film–substrate interface [19]. The observed insignificant interference oscillation for the substrate was due to the thickness of the ITO layer.

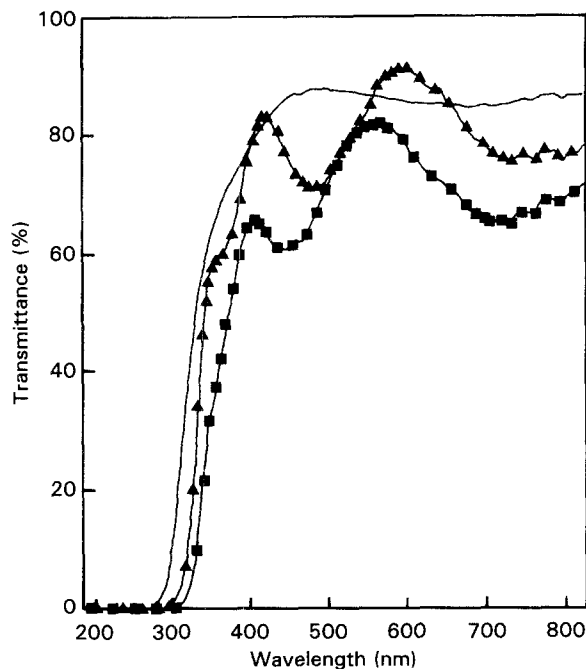


Figure 3 Transmittance spectra of (■) PE and (▲) PY samples; (—) ITO glass.

The thickness of the ITO layer used in this study was about 100 nm, well below the wavelength of visible light. The PY sample (10% perovskite phase content) and PE sample (90% perovskite phase content) show about 80 and 70% transmittance, respectively, with large interference oscillations. The observed large interference oscillation was due to the thickness of the PLZT thin film. The thickness of both films was about 500 nm and in the wavelength range of visible light. The PE sample with a relatively high perovskite phase content showed a lower transmittance. The interphase boundary serves as the light-scattering source when the refractive indices of the two phases are different. As the perovskite phase content increased, the interphase boundary increased between the perovskite and pyrochlore phases, and the light loss increased due to the scattering. The other possible cause of the observed lower transmittance for the PE sample was a higher surface reflectance, which depends on the refractive index of the material and affects the transmittance of the thin film. All three films showed ultraviolet absorption edges in the wavelength range of 260 to 320 nm. As the perovskite phase content increased, the wavelength at which the absorption edge occurred increased. The absorption represents electron transitions in the band gap, and the wavelength at which the absorption edge occurs represents the optical band-gap energy. The observed wavelength shift may indicate that the perovskite phase has a smaller band-gap energy than the pyrochlore phase.

Fig. 4 shows the polarization versus electric field ( $P$ - $E$ ) characteristics of the PLZT thin films heat-treated with two different heating schedules. The PE sample (Fig. 4a) exhibited a typical slim loop hysteresis in the  $P$ - $E$  curve. As reported in another study [20], PLZT of composition 9/65/35 shows a slim hysteresis loop and quadratic electro-optical behaviour. Quadratic electro-optic PLZT ceramics and thin

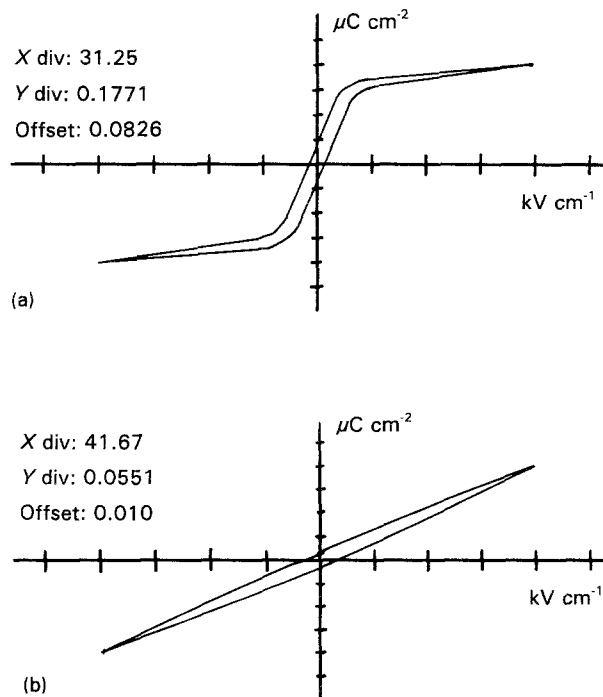


Figure 4 Polarization versus electric field curves of (a) PE and (b) PY samples.

films are potential materials for display applications. The remanent polarization and the coercive field were  $0.185 \mu\text{C cm}^{-2}$  and  $2.725 \text{ kV cm}^{-1}$  respectively. These values are still higher than the values observed for the bulk material, for which the values are close to zero. A tentative study is in progress to decrease the values and improve the other properties required for display applications. The resistivity of the PE sample was about  $5 \text{ G}\Omega\text{-cm}$ , which is similar to the resistivity values reported in another study [21].

A serious problem is often involved in measuring the electrical properties of sol-gel processed PLZT thin films. Several sputtered top Au electrodes were deposited on the thin film in this study. Some of them short-circuited to the bottom ITO electrode. Careful microstructural observation showed several micrometre-size voids, which may have arisen because the processing was not carried out in a clean environment and the voids probably served as a conducting path.

The PY sample (Fig. 4b) appeared to show a  $P$ - $E$  hysteresis but did not show saturation polarization within the limitations of the instrument used in this study. Because the pyrochlore structure is centrosymmetric [16], the pyrochlore phase is not ferroelectric and should neither show ferroelectric hysteresis nor saturation polarization. The observed hysteresis in the  $P$ - $E$  curve was probably due to the impedance mismatch between the thin film and the measuring circuit used in this study.

Fig. 5 shows the relative dielectric constant and the loss factor versus frequency ( $P$ - $f$ ) curves of the PLZT thin films heat-treated with two different heating schedules. The dielectric constant of the PE sample was about 90 up to 10 kHz, above which the dielectric constant decreased rapidly to a few units above 1 MHz. The dielectric constant at low frequency is lower than the values (several hundred) reported in

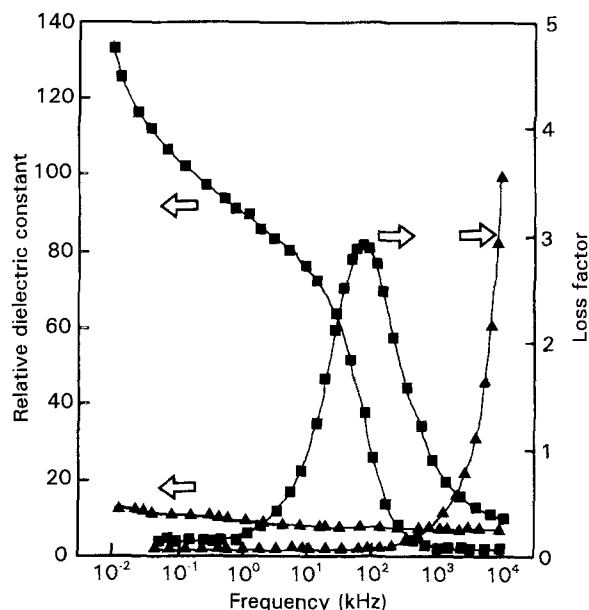


Figure 5 Relative dielectric constant and loss factor versus frequency curves of (■) PE and (▲) PY samples.

another study [22] in which a thin film having the same composition was sputtered on to a Pt substrate. The dielectric loss factor of the PE sample was about 0.2 below 1 kHz, above which the loss increased rapidly and showed a maximum near 100 kHz. The loss at low frequency is similar to the values reported by others [22]. The dielectric constant decrease and the loss increase in the frequency range between 10 kHz and 1 MHz were due to dispersion of the dipolar polarization of the permanent dipole moment in the ferroelectric perovskite phase. The frequency at which the dispersion occurs is two orders lower than that reported in another study [23] in which the composition (52/48) and the processing conditions were different from this study.

The dielectric constant of the PY sample was about 10 in the frequency range up to 1 MHz, above which the dielectric constant decreased. The dielectric constant of the PY sample was one order lower than that of the PE sample in the relatively low frequency range, which may indicate the absence of a permanent dipole moment in the non-ferroelectric pyrochlore phase because the PY sample consists of mainly pyrochlore phase. The dielectric loss factor of the PY sample was about 0.05 below 100 kHz, above which the loss increased rapidly. The loss of the PY sample is one order lower than that of the PE sample, corresponding to the larger band gap of the pyrochlore phase compared to the perovskite phase (Fig. 3). Because of the frequency limitations of the impedance analyser used in this study, the full range of the dispersion accompanying the large loss starting at 1 MHz was not measured, but it appears in Fig. 5 that the capacitance decrease rate for the PY sample was not as steep as that of the PE sample. The PY sample also consists of 10% ferroelectric perovskite phase, and this phase may show dispersion of the dipolar polarization of permanent dipole moment. Because the perovskite phase content was lower for the PY sample, the capacitance change during the dispersion was also

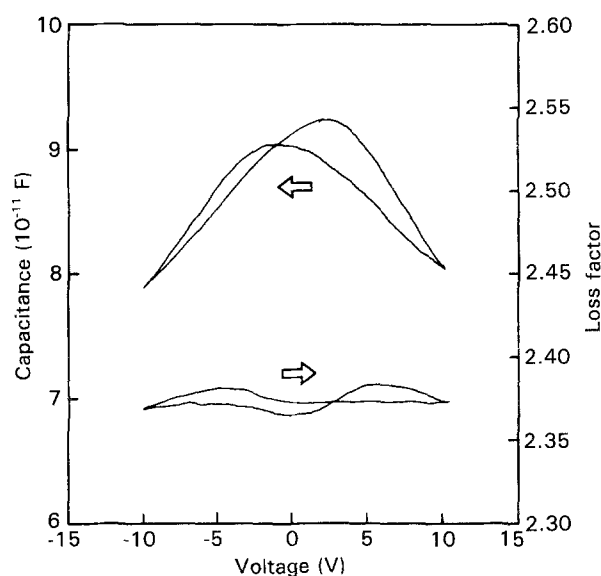


Figure 6 Capacitance and loss factor versus d.c. bias voltage curves of PE sample.

small. The frequency at which the dispersion occurred was two orders higher for the PY sample than for the PE sample. Further study is in progress to investigate these observations.

Fig. 6 shows the capacitance and loss factor versus d.c. bias voltage curves of a PE sample. The capacitance at zero bias voltage represents that with randomly oriented domains. As the positive and negative d.c. bias voltages increased and decreased, respectively, the domains were preferentially oriented to the bias field direction, the number of movable domains contributing to the capacitance decreased, and the capacitance decreased. The capacitance versus bias voltage curve also show hysteresis, representing the presence of ferroelectric domains.

#### 4. Summary

Sol-gel processed PLZT thin films consisting of two different perovskite phase contents were fabricated on ITO-coated glass substrates with two different heating schedules. The microstructure of the thin film heat-treated at 650°C for 30 min (PE sample) consists of about 90% perovskite phase, and that heat-treated at 500°C for 2 h (PY sample) consists of mainly pyrochlore phase and about 10% perovskite phase. The optical transmittances of PE and PY samples were 70 and 80%, respectively, and the transmittance spectra of both samples showed interference oscillation. The optical band-gap energy of the perovskite phase is relatively small compared to that of the pyrochlore phase. The thin film consisting of mainly perovskite phase (PE sample) showed a slim loop hysteresis in the polarization versus electric field curve and in the capacitance versus d.c. bias voltage curve, indicating the presence of ferroelectric domains, but the thin film consisting of mainly pyrochlore phase (PY sample) did not. The remanent polarization and coercive field were 0.185  $\mu\text{C cm}^{-2}$  and 2.725  $\text{kV cm}^{-2}$ , respectively. The dielectric constant and loss factor of the PE

sample were about 90 and about 0.2, respectively, at relatively low frequency and showed dispersion of the dipolar polarization of the permanent dipole moment in the ferroelectric perovskite phase in the frequency range between 10 kHz and 1 MHz.

### Acknowledgements

This work was supported by the Korea Ministry of Science and Technology.

### References

1. A. B. WEGNER, S. R. J. BRUECK and A. Y. WU, *Ferroelectrics* **116** (1991) 195.
2. T. KAWAGUCHI, H. ADACHI, K. SETSUNE, O. YAMAZAKI and K. WASA, *Appl. Opt.* **23** (1984) 2187.
3. C. A. PAZ de ARAUJO, L. D. McMILLAN, B. M. MELNICK, J. D. CUCHIARO and J. F. SCOTT, *Ferroelectrics* **104** (1990) 241.
4. M. OKUYAMA, T. USUKI, Y. HAMAKAWA and T. NAKAGAWA, *Appl. Phys.* **21** (1980) 339.
5. H. VOLZ, K. KOGER and H. SCHMITT, *Ferroelectrics* **51** (1983) 87.
6. M. ISHIDA, S. TSUJI, K. KIMURA, H. MATSUNAMI and T. TANAKA, *J. Cryst. Growth* **45** (1978) 393.
7. M. SAYER, in Proceedings of 6th IEEE International Symposium on Applications of Ferroelectrics, Bethlehem, June 1986, edited by V. E. Wood (IEEE, New York, 1986) p. 560.
8. D. S. YOON, J. M. KIM, K. C. AHN and K. NO, *Integrated Ferroelectrics* **4** (1994) 93.
9. K. D. BUDD, S. K. DEY and D. A. PAYNE, *Br. Ceram. Proc.* **36** (1985) 107.
10. S. KRISHNAKUMAR, S. C. ESENER, C. FAN, V. H. OZGUZ, M. A. TITLE, C. COZZOLINO and S. H. LEE, *MRS Symp. Proc.* **200** (1990) 91.
11. H. ADACHI, T. MITSUYU, O. YAMAZAKI and K. WASA, *J. Appl. Phys.* **60** (1986) 736.
12. Y. TAKAHASHI and K. YAMAGUCHI, *J. Mater. Sci.* **25** (1990) 3950.
13. C. C. HSUEH and M. L. MECARTNEY, *J. Mater. Res.* **6** (1991) 2208.
14. L. N. CHAPIN and S. A. MYERS, *MRS Symp. Proc.* **200** (1990) 153.
15. G. YI, Z. WU and M. SAYER, *J. Appl. Phys.* **64** (1988) 2717.
16. C. K. KWOK and S. B. DESU, *Ceram. Trans.* **25** (1992) 73.
17. T. MIHARA, H. WATANABE, H. YOSHIMORI, C. A. PAZ de ARAUJO, B. MELNICK and L. D. McMILLAN, *Integrated Ferroelectrics* **1** (1992) 209.
18. H. HU, L. SHI, V. KUMAR and S. B. KRUPANIDHI, *Ceram. Trans.* **25** (1992) 113.
19. K. NASSAU, "The Physics and Chemistry of Colors" (Wiley, New York, 1983) p. 427.
20. S. L. SWARTZ, *IEEE Trans. Elec. Ins.* **25** (1990) 935.
21. H. N. AL-SHAREEF, K. D. GIFFORD, M. S. AMEEN, S. H. ROU, P. D. HREN, O. AUCIELLO and A. I. KINGON, *Ceram. Trans.* **25** (1992) 97.
22. M. ISHIDA, H. MATSUNAMI and T. TANAKA, *J. Appl. Phys.* **48** (1977) 950.
23. A. GUPTA and S. K. DEY, *Ceram. Trans.* **25** (1992) 243.

Received 26 January 1993  
and accepted 21 March 1994